ACS Catalysis

Open Access
This article is licensed under CC-BY-NC-ND 4.0

pubs.acs.org/acscatalysis
Perspective

The Conundrum of "Pair Sites" in Langmuir–Hinshelwood Reaction Kinetics in Heterogeneous Catalysis

Daniyal Kiani* and Israel E. Wachs*

Cite This: *ACS Catal.* 2024, 14, 10260–10270
Read Online

ACCESS | Metrics & More | Article Recommendations

ABSTRACT: Understanding reaction kinetics is crucial for designing and applying heterogeneous catalytic processes in chemical and energy conversion. Here, we revisit the Langmuir–Hinshelwood (L-H) kinetic model for bimolecular surface reactions, originally formulated for metal catalysts, assuming immobile adsorbates on neighboring pair sites, with the rate varying linearly with the density of surface sites (sites per unit area); $r \propto [*]_o^1$. Supported metal oxide catalysts, however, offer systematic control over $[*]_o$ through variation of the active two-dimensional metal oxide loading in the submonolayer region. Various reactions catalyzed by supported metal oxides are analyzed, such as supported VO_x catalysts, including methanol oxidation, oxidative dehydrogenation of propane and ethane, SO_2 oxidation to SO_3, propene oxidation to acrolein, *n*-butane oxidation to maleic anhydride, and selective catalytic reduction of nitric oxide with ammonia. The analysis reveals diverse dependencies of reaction rate on $[*]_o$ for these surface reactions, with $r \propto [*]_o^n$, where n equals 1 for reactions with a unimolecular rate-determining step and 2 for those with a bimolecular rate-limiting step or exchange of more than 2 electrons. We propose refraining from a priori assumptions about the nature and density of surface sites or adsorbate behavior, advocating instead for data-driven elucidation of kinetics based on the density of surface sites, adsorbate coverage, etc. Additionally, recent studies on catalytic surface mechanisms have shed light on nonadjacent catalytic sites catalyzing surface reactions in contrast to the traditional requirement of adjacent/pair sites. These findings underscore the need for a more nuanced approach in modeling heterogeneous catalysis, especially supported metal oxide catalysts, encouraging reliance on experimental data over idealized assumptions that are often difficult to justify.

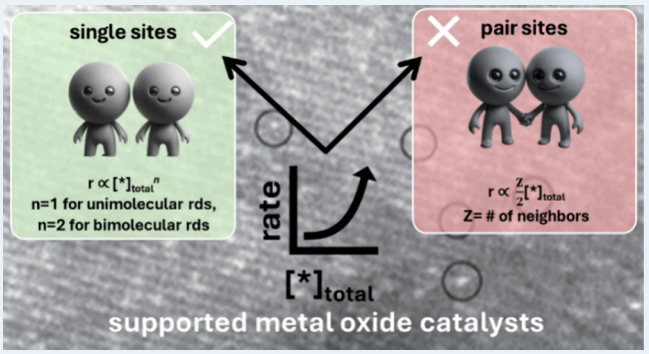

KEYWORDS: *surface mechanism, mean-field approximation, adjacent sites, metal oxide catalysts, supported vanadium oxide, oxidations*

1. INTRODUCTION

The kinetic assessment of reactions is essential to the design and application of heterogeneous catalytic processes employed in chemical and energy conversion. One of the most invoked kinetic models for surface bimolecular reactions is the Langmuir–Hinshelwood (L-H) model, later modified by Hougan and Watson and popularized as the Langmuir–Hinshelwood–Hougan–Watson (L-H-H-W) model.[1] The L-H and L-H-H-W models are both based on the Langmuir isotherm, which was obtained on the following assumptions associated with an ideal uniform surface—assumptions we now categorically know to not apply for all realistic heterogeneous catalysts investigated since Langmuir's work:

1. Localized adsorption occurs only on vacant surface sites.
2. Only one adsorbed species can exist per surface site.
3. The heat of adsorption is constant and independent of surface coverage, which assumes that no lateral interaction occurs between the adsorbed species.

Subsequent modifications to the idealized Langmuir isotherm describing the adsorption–desorption equilibrium introduced further nuances into the simple mathematical expression that are now ubiquitous in textbooks and papers discussing heterogeneous chemical kinetics and catalysis. One of the major modifications made to the Langmuir isotherm equation stems from the idea of the recombinative desorption of dissociatively adsorbed species to account for two distinct possibilities:

1. Recombinative desorption of *mobile* adsorbates that easily diffuse on the solid surface. This is the simpler case in terms of mathematical description as the associative

Received: May 11, 2024
Revised: June 12, 2024
Accepted: June 12, 2024
Published: June 21, 2024

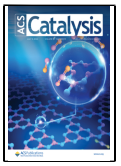

© 2024 The Authors. Published by American Chemical Society

desorption rate depends only on the surface concentration/coverage of the adsorbates.

2. Recombinative desorption of *immobile* adsorbates such that the adsorbates are strongly tethered to the adsorption sites and do not have any lateral degree of freedom. In this scenario, associative desorption can only occur if the two dissociated adsorbates are adjacent to each other on "pair sites".[1,2] The requirement for pair sites introduces a new parameter "Z" into the model, derived by application of statistical equilibrium, to account for the number of nearest neighbor surface sites $\left(\frac{Z}{2}/[*]_o^{\,1}\right)$.

From the early days of the derivation of the L-H model, the assumption of immobile adsorbates on neighboring pair sites, usually arranged in a square lattice, has been introduced into the literature, implicitly or explicitly.[1,3,4] Noting the above context regarding the assumptions behind the L-H mechanism, we next look at the L-H model and what these assumptions mean from an experimental standpoint. In its simplest form, the L-H mechanism for a bimolecular reaction is as follows: R_1 and R_2 are reversibly adsorbed on vacant surface sites, [*], to form adsorption complexes R_1* and R_2*. The adsorbates transform irreversibly via a slow reaction step between R_1* and R_2* to yield product P that does not adsorb on the surface, and the remaining vacant surface sites are free to adsorb more reactant molecules.

$$R_1 + [*] \rightleftarrows [R_1^*] \tag{1}$$

$$R_2 + [*] \rightleftarrows [R_2^*] \tag{2}$$

$$[R_2^*] + [R_1^*] \rightarrow P + 2[*]\ (\text{rate-determining step}) \tag{3}$$

where the surface site balance is given by

$$[*]_o = [*] + [R_1^*] + [R_2^*] \tag{4}$$

with $[*]_o$ representing the surface site density, i.e., total number of surface sites per unit area accounting for both vacant and occupied sites. K_{R1} and K_{R2} are equilibrium adsorption rate constants describing the adsorption−desorption of the reactants, while k_{rds} is the Arrhenius rate constant for the rate-determining step 3. The above details result in the kinetic eq 5 that relates the rate of production of product P (dP/dt) as

$$\therefore\ dP/dt = \frac{k_{rds}\cdot K_{R1}\cdot K_{R2}\cdot P_{R1}\cdot P_{R2}\cdot [*]_o^{\,2}}{(1 + K_{R1}\cdot P_{R1} + K_{R2}\cdot P_{R2})^2} \tag{5}$$

Note, we do not specify a priori if the adsorbates R_1* and R_2* are mobile or immobile, and thus, no special site requirement, such as the presence of pair sites with Z nearest neighbors, is necessary. In this form, the rate of the reaction for the rate-determining step depends on two surface sites and, thus, will exhibit second-order dependence with respect to the total number of surface sites of the solid catalyst.

However, a second school of thought also exists that derives the L-H mechanism with the a priori assumption of immobile adsorbates on pair sites on a perfect square lattice with Z nearest neighbors. In this case, the surface $[R_1^*]$ and $[R_2^*]$ intermediates are required to be adjacent to each other to react and form P, and if not, they are assumed to be kinetically irrelevant. This school of thought, championed by luminaries like Hougen, Watson, and Boudart, originated in the early days of heterogeneous catalysis when kinetics of *metal* catalysts were studied almost exclusively and the kinetics of supported metal oxide catalysts had received little attention.[3,5,6] Supported metal oxide catalysts consist of surface metal oxides completely dispersed on an oxide support that represent the catalytic active surface sites.[7] The fundamentals and derivation from this point of view, encompassing pair sites and lattice statistical equilibrium, can be found in many textbooks, referenced herein for the reader's convenience.[4,8] A unique outcome of the a priori assumption of immobile adsorbates on pair sites is that the higher order dependence of the L-H reaction rate on the number density of surface sites is reduced to a value of 1 as only "pair sites" can serve as the two sites for immobile adsorbates. Under this viewpoint, the reaction rate will be proportional to $\frac{Z}{2}[*]_o^{\,1}$, as opposed to $[*]_o^{\,2}$, where Z is the number of nearest neighbors for surface bimolecular reactions, as stated earlier, and $[*]_o$ is the surface site density (surface sites per unit area), which Boudart denotes as "[L]" in his derivation.[3,4] This point has been explicitly highlighted by Boudart,[3,4] and subsequently by his former students like M. A. Vannice,[9] and Davis and Davis[10] in their own textbooks. This a priori assumption of immobile adsorbates on adjacent pair sites is also the basis of the mean field approximation often invoked when discussing the kinetics of bimolecular reactions. For example, surface A* and surface B* react to form product C, where the rate of formation of C would be equal to $[*]_o k\theta_A\theta_B$ instead of $[*]_o^{\,2} k\theta_A\theta_B$.[11] In the mean-field approximation, surface A* and surface B* are assumed to be distributed randomly over adjacent sites (e.g., pair sites that can accommodate surface A* and surface B* together).[11]

Prima facie, the difference in the two L-H derivations is minor; however, the outcome from an experimental standpoint is profound. The former derivation indicates that, in certain cases for surface bimolecular reactions, the reaction rate will exhibit a higher-order dependence on the *total* number density of surface sites, $[*]_o$, e.g., rate $r \propto [*]_{total}^{\,n}$ where $n > 1$. This further implies that kinetic analysis may allow differentiating between surface mechanisms based on the site requirements. For instance, the dependence of the rate on $[*]_o$ can be used to distinguish between a bimolecular reaction occurring via the Eley−Rideal (E-R) vs L-H mechanism, as the E-R mechanism is limited to only one possibility under the kinetic regime since it is a reaction between a nonchemisorbed specie with a chemisorbed specie that results in $r \propto [*]_o^{\,1}$. On the other hand, the reaction rate in L-H surface bimolecular reaction mechanisms can exhibit higher-order dependence on $[*]_o$ such as $r \propto [*]_o^{\,2}$ (as indicated in eq 5 above). According to the pair site assumption in the latter derivation of the L-H model, kinetic analysis based on rate vs $[*]_o$ cannot be reliably used to distinguish between L-H and vs E-R mechanisms as both will yield the same linear dependence under certain simplifying circumstances.[4]

In the next sections, we discuss the caveats of first-order versus higher-order dependence of the experimentally measured reaction rates on $[*]_o$ using examples from the literature on supported metal oxide catalysts from our group as well as other groups. We show that the a priori assumption of immobile adsorbates on adjacent/pair sites for supported metal oxide catalysts is not necessary and the expected linear dependence of reaction rates on $[*]_o^{\,1}$, applied for metal catalysis, can be violated. We provide various literature examples of reactions catalyzed by supported metal oxide catalysts evincing up to a second-order dependence of reaction rate on $[*]_o$. For other reactions, the exact same catalysts exhibit a first-order dependence; the underlying mechanistic reason behind the variation of reaction rate dependence on $[*]_o$ for different reactions over the same catalyst is also discussed below. Our

https://doi.org/10.1021/acscatal.4c02813
ACS Catal. 2024, 14, 10260−10270

objective through this Perspective is to highlight the complexities of supported metal oxide catalysts and differentiate how models such as L-H/L-H-H-W—based on metal catalysts—should be applied to supported metal oxide catalysts in order to determine the number of participating sites in a catalytic mechanism and to prevent confusion and controversy.

2. EVIDENCE OF MOBILE ADSORBATES ON NONADJACENT SITES IN HETEROGENEOUS CATALYSIS

2.1. Metal Catalysts. Although assuming immobile adsorbates on pair sites arranged in a regular lattice produces a useful mathematical model that has been ubiquitously adopted for kinetic reaction models across heterogeneous catalysis, it must be noted that this assumption has not been experimentally confirmed when it comes to most solid catalysts, including metal catalysts. For example, in a series of elegant papers utilizing scanning tunneling microscopy (STM) of solid catalysts, published during the 1980s−1990s, Ertl and co-workers unequivocally showed that surface adsorbates, even on single crystal metal catalysts, were mobile and significantly diffused. Specifically, as shown in Figure 1 left, NO dissociation over

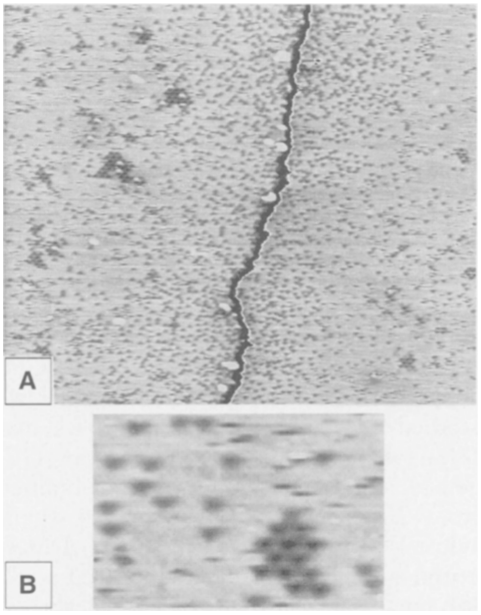

Figure 1. STM images of Ru(0001) after dissociation of 0.3 L of NO at 315 K. (A) 380 × 380 Å STM image showing two terraces, upper one on the left hand side of the panel and a lower one on the right hand side of the panel, with a monatomic step shown as a darker gray stripe. Individual atoms of N and islands of O atoms can be seen at a significant distance from the step sites that serve as the active sites for this dissociative adsorption. (B) 60 × 40 Å zoomed-in section from (A) showing an island of O atoms formed via fast diffusion of O atoms on the surface. The individual atoms around the island of O atoms are N atoms. Figure adapted with permission from ref 12. Copyright 1996 American Association for the Advancement of Science.

Ru(0001) evinced that, although the dissociation occurred only at surface step sites, surface O atoms rapidly diffused a long distance away from the step sites and formed surface O islands.[12] On the other hand, N atoms on the surface also diffused, but to a lesser degree, and were observed in proximity of the step sites that were deemed the surface active sites. Note, this reaction would typically be thought of as NO dissociating over two adjacent [*] sites to form immobile surface O* and N* adsorbates.[12] However, the direct evidence from *in situ* STM studies suggests otherwise and reveals a more complicated picture. Moreover, STM also shows that the surface adsorbates, formed via dissociative adsorption of the substrate, are extremely "mobile" and not statically tethered to any fixed pair sites even at low temperatures on a single crystal surface. In the real-world, supported metal catalysts operating at steady state reaction conditions of high substrate conversions and high temperatures will arguably experience greater surface diffusion of the adsorbates, as well as diffusion and dynamic restructuring of the surface sites, which means that the nature and distribution of active surface sites and the surface adsorbates will be even further from the idealized assumptions by Hougen and Watson.[1,2]

Although direct experimental evidence clearly refutes the idealized assumptions of regularly arranged pair sites, we note that this idea stems out of studying metal catalysts: unsupported metal surfaces during the first half of the twentieth century, followed by supported metals and single crystal metals in the second half of the twentieth century. In metal catalysts, the density of surface sites (total sites per unit area) cannot be varied since the surface site ensembles are fixed by the crystal morphology, and thus, studies from this period often derive and rationalize the data in terms of fractional surface coverage (θ) of pair sites in the context of single crystal lattice statistics. It was not until much later that rigorous methods to count the total number of active sites were devised and popularized by Boudart and others.[4] Even with the introduction of chemisorption techniques to count the number of surface sites in metal catalysts in order to calculate turnover frequencies,[3,4] it remained impossible to systematically and quantifiably *vary* the total number and arrangement of surface sites on metal surfaces since the surface density of the metal atoms is fixed at $\sim 1 \times 10^{15}$ sites/cm^2.[3,4] Therefore, experimental validation of the dependence of the reaction rate on the density of surface sites remained out of experimental reach, and the assumption of the rate linearly depending on the concentration of pair sites was assumed to be valid. In the last two decades of the twentieth century, however, supported metal oxide catalysts appeared on the scene and allowed one to introduce a systematic way to vary the number density of surface sites $[*]_o$ by varying the active surface metal oxide loading on the support since the surface metal oxides are typically completely dispersed below monolayer coverage for many catalyst systems. In the next section, we focus on the supported metal oxide literature to revisit the assumptions behind the L-H mechanism.

2.2. Supported Metal Oxide Catalysts. The assumption of a "regular geometric pattern determined by the lattice structure" of the "pair/adjacent sites" is not experimentally supported when it comes to most solid catalysts, especially supported metal oxides. Numerous studies have shown that a submonolayer and monolayer of transition metal oxides can be supported on various oxide supports, forming unique amorphous/disordered two-dimensional structures that remain a function of the active metal oxide loading and the support's surface hydroxyl density/reactivity, as opposed to a function of the lattice arrangement of the catalyst support. As suggested by the HAAD-STEM images of zirconia-supported tungsten oxide (WO_x/ZrO_2) in Figure 2a, at low loadings (e.g., submonolayer coverage), isolated surface WO_x sites are prevalent, while at higher loadings, as monolayer coverage is approached, oligomeric surface $(WO_x)_n$ sites form.[13] Above monolayer

https://doi.org/10.1021/acscatal.4c02813
ACS Catal. 2024, 14, 10260−10270

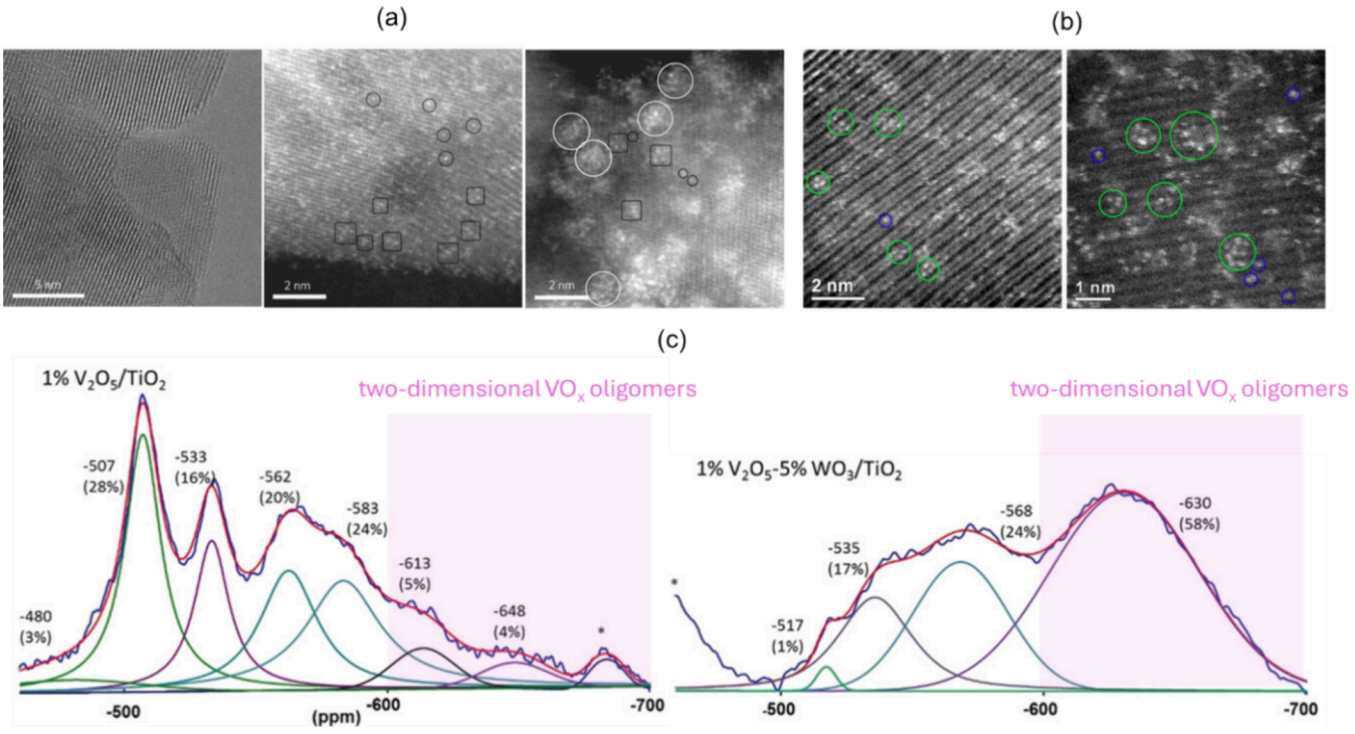

Figure 2. (a) Aberration-corrected STEM-HAADF images of bare ZrO_2 support, 2.9% WOx/ZrO_2, and 6.2% WO_x/ZrO_2. Black circles highlight the presence of single tungsten atoms corresponding to surface monotungstate sites, and the black squares highlight surface polytungstate sites with several tungsten atoms linked by oxygen bridging bonds. White circles indicate WO_x clusters with diameters of 0.8−1.0 nm. These clusters were found only in samples with a surface density above monolayer coverage. Images adapted with permission from ref 13. Copyright 2009, Springer Nature. (b) Aberration-corrected STEM-HAADF images of 5% WO_x/ZrO_2 and 7% WO_x/TiO_2 catalysts, evincing similar WO_x structures on the surface of ZrO_2 and TiO_2 supports despite unique lattices of the supports. The green circles in this case identify surface WO_x oligomers, while the blue circles identify the isolated WO_x sites. Adapted with permission from ref 17. Copyright 2012, Elsevier. (c) Magic angle spinning NMR of supported surface 1% VO_x/TiO_2 catalysts in the absence and presence of 5 %WO_x promoter, evincing a drastic increase in surface VO_x oligomers upon WO_x promotion, corroborating that the TiO_2 lattice primarily does not control surface VO_x speciation. Figure adapted with permission from ref 18. Copyright 2019, John Wiley and Sons.

coverage, three-dimensional WO_3 clusters form.[13] It has been further shown that monolayer coverage of a surface metal oxide, such as vanadium oxide (VO_x) or WO_x or molybdenum oxide (MoO_x), can be formed on oxide supports possessing vastly different lattices including ZrO_2, Al_2O_3, TiO_2, Nb_2O_5, etc. that yield similar surface sites comprising oligomeric structures of the supported metal oxide conjoined via metal—O—metal bonds, with constant surface atom density independent of oxide supports (e.g., 8 V atoms nm^{-2} for VO_x monolayer, 4.5 W atoms/nm^2 for WO_x, and 4.5 Mo atoms/nm^2 for MoO_x monolayers).[7,14] On the other hand, supports like SiO_2 cannot be used to synthesize a complete surface metal oxide monolayer catalyst since only submonolayer catalysts can be achieved using SiO_2 at low weight loadings of the metal oxide, where each surface WO_x or VO_x site tends to be atomically isolated and no metal—O—metal linkages are present.[15,16] A representative example is shown in Figure 2b, where a submonolayer of surface WO_x supported on ZrO_2 and TiO_2 are investigated via HAAD-STEM. Despite the obviously different lattice structures of the catalyst supports, the surface WO_x sites are similar in both cases: two-dimensional and randomly distributed. In both cases, a mixture of oligomeric and isolated monomeric WO_x sites is observed that neither are arranged in regular geometric patterns nor contain distinct pair sites. Although not shown herein, Raman and X-ray absorption (XAS) spectroscopies have also elucidated the molecular structures of the surface WO_x sites as a function of loading, and curious readers are directed to the body of work cited herein and references within. It suffices to note that, when isolated, surface WO_x sites can be present as digrafted, dioxo $[_2(O—)W(=O)_2]$ or tetra-grafted, mono-oxo $[_4(O—)W(=O)_1]$.[15−17] When present as oligomers, the surface WO_x is a chain of interlinked mono-oxo units. Lastly, in Figure 2c, we show solid-state high field ^{51}V magic angle spinning NMR of 1% VO_x/TiO_2 as a function of the WO_x promoter.[18] Yet again, despite both samples having the identical TiO_2 support and VO_x loadings, it is seen that the surface VO_x structures are significantly influenced by the presence of the surface WO_x promoter, the addition of which causes surface crowding, subsequently leading to an increase in the local population of surface VO_x oligomers[18]—an example of the complexity of surface sites in supported metal oxide catalysts and the unique opportunity they present to systematically vary the total number of surface active sites at the local level.

Another important point to note regarding supported metal oxides is that, in general, the surface metal oxide sites and the surface adsorbates formed during reaction are *mobile*. It is well-known that surface diffusion or migration of surface metal oxide sites play an important role in agglomeration, sintering, and active-component redistribution in heterogeneous catalysts.[19−27] Thermally driven diffusion leads to significant surface migration or diffusion of one component over the surfaces of an oxide support, and high temperature and presence of surface adsorbates can further help overcome the activation barrier for surface diffusion.[27,28] As a rule, if the temperatures are higher

https://doi.org/10.1021/acscatal.4c02813
ACS Catal. 2024, 14, 10260−10270

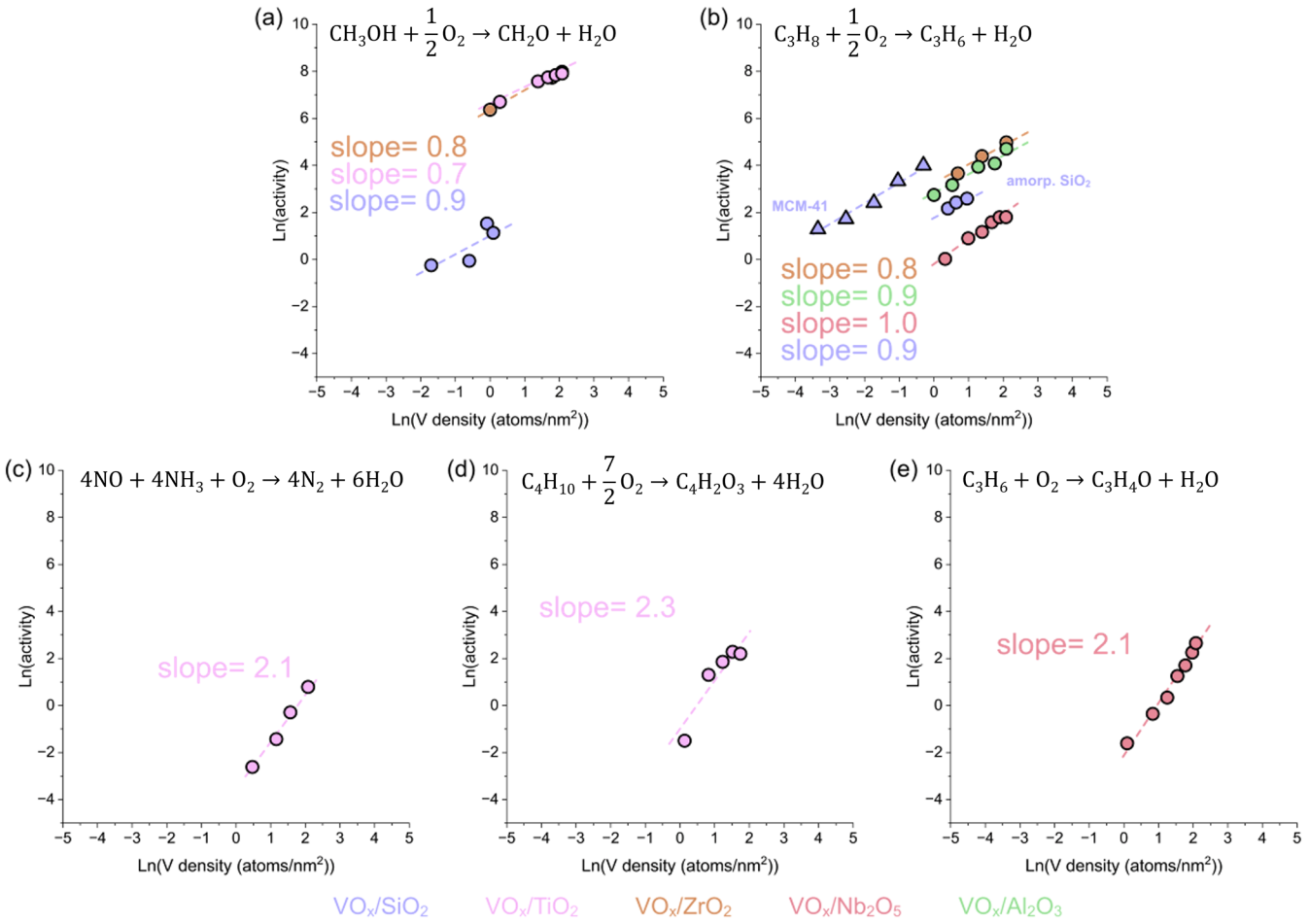

Figure 3. Ln-Ln plot of activity ($mmol_{reactant}\ g_{cat}^{-1}\ hr^{-1}$) vs V density (atoms nm^{-2}) of supported VO_x catalysts for: (a) methanol oxidation to formaldehyde at 230 °C, data originally reported in ref 80, (b) oxidative dehydrogenation of propane to propene at 350−475 °C, data originally reported in refs 44, 81, 82, (c) selective catalytic reduction of NO with NH_3 (standard SCR) at 200 °C, data originally reported in ref 18, (d) *n*-butane oxidation to maleic anhydride at 221 °C, originally reported in ref 46, and (e) propylene oxidation to acrolein at 300 °C, originally reported in ref 72. In each Ln-Ln plot, the slope of the linear fit is shown. Supported VO_x on various oxides are shown as different colored data points; SiO_2 in purple, TiO_2 in pink, ZrO_2 in orange, Nb_2O_5 in salmon, and Al_2O_3 in green. All data used herein were collected under steady state differential reaction conditions at low reactant conversions.

than the Tammann temperature (the temperature when surface atoms begin to diffuse) of the supported metal oxide, surface diffusion is expected to occur at an appreciable rate.[23,25] Given that steady state temperatures, especially for reactions discussed herein, are in the range of 200−500 °C, this requirement is satisfied as the Tammann temperature of bulk V_2O_5 is 200−210 °C, while that of the surface VO_x may be slightly higher or lower.[25,29−31] For instance, the barrier for surface diffusion of VO_x in VO_x/TiO_2 was estimated to be merely ∼40 kJ mol^{-1}, where the barrier magnitude depends on various underlying factors including the oxidation state of the V species.[32,33] In contrast, activation barriers for catalytic reactions may vary from ∼80 to 160 kJ mol^{-1},[34−38] while diffusion barriers for adsorbates can be in the range of ∼10−50 kJ mol^{-1}.[39−41] Therefore, surface diffusion of active metal oxide sites (VO_x) and surface adsorbates is expected to be significant at conditions where the catalytic reaction steps occur, which usually have larger activation barriers, indicating that both the surface active sites and adsorbates will be *mobile* under reaction conditions.

In summary, multiple reports from many groups have shown that the above-mentioned assumptions made in the derivation of the L-H model regarding the *regular pattern* of *pair sites* that can accommodate *immobile surface adsorbates* do not need to be invoked for supported metal oxide catalysts, where both surface active sites and adsorbates are known to be mobile. Moreover, the broader literature on supported metal oxide catalysts has rigorously shown that the total number of surface active sites at the local level can be systematically varied either by varying the weight % loading of the metal oxide on the support such that surface coverage varies between ∼0 < monolayer ≤ 1[34,42−51] or by introducing a promoter that increases the local surface site density by crowding while keeping the surface active metal oxide content constant.[15,16,18]

3. UNDERSTANDING REACTION RATE DEPENDENCE ON THE NUMBER OF PARTICIPATING ACTIVE SITES IN HETEROGENEOUS CATALYSIS

For the purpose of this discussion, we focus on supported VO_x catalysts, although the points noted here are applicable to other submonolayer supported metal oxide catalysts as well. It is known that the number of catalytic active surface VO_x sites per catalyst mass increases linearly with VO_x loading in the submonolayer region, where the VO_x is 100% dispersed on the oxide support. Therefore, supported metal oxide catalysts

https://doi.org/10.1021/acscatal.4c02813
ACS Catal. 2024, 14, 10260−10270

allow for fine control over the density of surface sites, by controlling the metal oxide loading below monolayer coverage, and thus, they are uniquely suited to test the validity of the assumptions behind the L-H model. Herein, we summarize two sets of literature bodies, such that the first set evinces that reaction rate linearly varies with $[*]_o$, while the second set suggests that the rate varies quadratically with $[*]_o$. We show that in fact the reaction rate is dependent on the demands of the specific reaction and the site requirement of the rate-determining step: single site vs multiple sites. Therefore, our analysis clearly indicates that a more accurate interpretation would be rate $r \propto [*]^n$, where n is the site requirement of the rate-determining step and can range from 1 to 2.

$r \propto [*]_o^1$. In Figure 3a,b, we plot the natural log of activity—molar rate of reactant conversion normalized per time, per gram of catalyst—against the natural log of the surface vanadium density in atoms per nm^2 for partial oxidation of methanol to formaldehyde and oxidative dehydrogenation of propane to propylene, respectively, catalyzed by supported VO_x catalysts. Both of these reactions require only one oxygen atom and, thus, involve the transfer of two electrons from the surface VO_x to complete the catalytic cycle. In both instances, the rate-determining step is unimolecular, involving a single active surface VO_x site. In the case of methanol oxidation, the rate-determining step involves dehydrogenation of the C−H bond of surface methoxy (CH_3O^*) to formaldehyde.[14,52,53] Likewise, the rate-determining step in the oxidative dehydrogenation of propane involves C−H scission.[34,54−56] In both reactions, the rate-determining step is found to be zero-order with respect to gaseous molecular oxygen, indicating that gas phase molecular O_2 is not participating in that rate-determining step, and the oxygen involved is present in the single surface VO_x catalytic site participating in the slow step.[36,53,57−59] Therefore, despite the apparent bimolecular stoichiometry of the reactions, the Ln-Ln plots of methanol oxidation (Figure 3a) and oxidative dehydrogenation of propane (Figure 3b) clearly indicate a slope of ∼1 for various supported VO_x catalysts, evincing that the rate is linearly correlated with VO_x surface density, i.e., $r \propto [VO_x]_o^1$.[34,47,60−63] These plots also show that this conclusion can be generalized for supported VO_x catalysts, as all analyzed supported catalysts, irrespective of the support identity, show a linear dependence owing to the identical rate-determining step.[64] Similarly, the linear correlation between catalytic activity of supported metal oxides, including supported VO_x, with metal oxide surface density (or the metal oxide weight loading) has also been shown for other oxidation reactions requiring only one O atom or two electrons (e.g., SO_2 oxidation to SO_3[65] and oxidative dehydrogenation of C_2H_6 to C_2H_4).[66] Furthermore, the linear increase in catalytic activity with surface VO_x loading for these reactions demonstrates that there is no difference in activity between isolated and oligomeric surface VO_x sites on the same support for all oxide supports.

$r \propto [*]_o^2$. Oxidation reactions requiring more than one O atom or two electrons, however, require multiple surface VO_x sites since V is only able to give one O atom and reduces to V^{+3}.[67,46] The Ln-Ln plots of the catalytic activity vs surface vanadium density for various supported VO_x catalysts are shown in Figure 3c−e. These reactions, namely, selective catalytic reduction of NO with NH_3 (Figure 3c), oxidation of *n*-butane to maleic anhydride (Figure 3d), and oxidation of propylene to acrolein (Figure 3e) are chosen because the rate-determining step involved in each of these reactions necessitates the involvement of at least two surface VO_x sites. In these reactions, the rate-determining step may be nonzero-order with respect to gaseous molecular O_2, but the oxygen dependence can appear zero-order depending on the operating conditions of temperature, conversion, and O_2 partial pressures (SCR,[68,69] butane oxidation to maleic anhydride,[70,71] propylene oxidation to acrolein[72,73]), indicating that active site reoxidation may become kinetically relevant in such cases. The site dependence for the standard selective catalytic reduction of NO with NH_3, where VO_x/TiO_2 catalysts are commercially employed at the present, is shown in Figure 3c. It has been shown that the rate-determining step involves breaking of an N−H bond during formation or decomposition of the bimolecular $[ON{-}NH_x]$ reaction intermediate complex.[35,74] Noting the bimolecular nature of the rate-determining step where two surface sites are expected to be involved, it is not surprising that the Ln-Ln plot exhibits a slope of ∼2.[18] Likewise, the rate-determining step in the case of *n*-butane oxidation to maleic anhydride is known to be multinuclear with both surface acid sites and surface redox sites participating in slow steps involving olefin production and the subsequent butadiene oxidation, respectively,[46,75−78] which is reflected in the slope of the Ln-Ln plot being 2. Lastly, propylene oxidation to acrolein proceeds via a pathway with bimolecular rate-limiting step(s) involving C−H bond breaking of the surface allyl intermediate and O* insertion into the surface allyl intermediate, which may be a concerted reaction step occurring simultaneously.[38,72,79] In agreement, the slope of the Ln(activity) vs Ln(surface V density) plot is ∼2, indicating the involvement of two surface VO_x active sites in the rate-determining step. In the three cases discussed above, two catalytic sites are involved in the slow step, and therefore, the reaction rate exhibits second-order dependence on $[*]_o$ ($r \propto [VO_x]_o^2$).

The examples discussed in these sections highlight the following key points:

(i) Unlike supported metal catalysts and single crystal metal catalysts with metal surface density fixed at $\sim 1 \times 10^{15}$ sites cm^{-2}, supported metal oxide catalysts allow fine control over density of surface sites via control of the metal oxide loading up to monolayer surface coverage. This allows the use of supported metal oxide catalysts (such as supported VO_x) for various catalytic reactions in order to probe the dependence of the reaction rates on the density of surface VO_x sites in the submonolayer region.

(ii) The dependence of the reaction rate on surface density of sites cannot be fixed or predicted a priori based on the global stoichiometry of a reaction, as this dependence is reliant upon the site requirements of the rate-determining step in the catalytic reaction mechanism.

(iii) For a wide range of reactions catalyzed by supported VO_x catalysts, the rate exhibits varying dependence on the $[*]_o^n$ term, where *n* is 1 for reactions involving a unimolecular rate-determining step and 2 for reactions involving a surface bimolecular rate-determining step or two separate sites participating in two slow steps.

(iv) If the pair site assumption in the L-H model, discussed in preceding sections, was indeed valid, Ln(activity) vs $Ln[*]_o$ would never exceed a slope of 1. However, the studies highlighted herein clearly show that a slope of ∼2 is routinely observed for multiple reactions. Therefore, this a priori assumption of immobile adsorbates on immobile/static pair sites does not appear to hold for supported metal oxide catalysts. Furthermore, supported

https://doi.org/10.1021/acscatal.4c02813
ACS Catal. 2024, 14, 10260−10270

metal oxide catalysts contain mobile surface adsorbates and metal oxide sites that diffuse on the support surface during reaction. As noted above, the surface diffusion barrier of supported metal oxides, especially supported VO_x, is merely ∼40 kJ mol^{-1} at circa room temperature,[32,33] and the Tammann temperature of V_2O_5 is ∼200−210 °C.[25,29−31] On the other hand, activation barriers for the slow reaction step(s) are often two to four times larger in magnitude than the diffusion barrier of surface VO_x sites, and the reaction temperatures are in the range of 200−500 °C (e.g., reaction temperature ≥ Tammann temperature), indicating that under reaction conditions the surface VO_x sites will easily diffuse. Involvement of mobile sites and mobile adsorbates can lead to nonlinear correlations between reaction rate and $[*]_o$, since the probability (and frequency) of effective collisions between two adsorbates/sites scales nonlinearly with $[*]_o$. Alternatively, if the adsorbates and sites were *immobile* and, therefore, the two-site rate-determining step could only occur on adjacent pair sites, the density of adjacent sites (aka pair sites) may exhibit a second-order dependence on the density of total surface sites (e.g., $[**] \propto [*]_o^2$). However, an important caveat of square dependence of pair site surface density on total surface site density is the adherence to Henry's law limit; infinite (or at least ample) dilution of surface sites is necessary. In other words, in the limit of approaching a full monolayer (surface saturation limit), the density of pair surface sites should exhibit much less than second-order dependence on the density of total surface sites. Experimentally, this is *not* the case in the studies discussed above. In the data plotted in Figure 3, going from near zero VO_x surface coverage to a full monolayer (∼8 $V_{atoms}nm^{-2}$), supported VO_x catalysts exhibit a slope of ∼2 and a goodness of fit, r^2, value >0.90 for all cases (>0.98 for SCR and propene oxidation, 0.90 for butane oxidation). If the second-order dependence was shifting to a subsecond order dependence as the monolayer coverage was approached, r^2 of the fit in Ln-Ln plots would have decreased significantly since half of the data points are in the 0.5 > monolayer ≤ 1 surface coverage range. Therefore, we propose that the involvement of immobile pair sites with immobile adsorbates is highly unlikely considering the aforementioned experimental data and corresponding fits and that the second-order dependence of the reaction rate on surface site density is a consequence of the rate-determining step(s) requiring two surface sites, both adsorbates and sites being mobile.

(v) Here, it is also valuable to briefly note that reaction rate exhibiting first- or second-order dependence on the surface site density also has bearing on how kinetic data are interpreted in the context of transport limitations. For example, the Koros-Nowak criterion and the Madon-Boudart test (mostly applicable to supported metal catalysts as specified by the original authors)[83] both check for the following: if the number of catalytic sites are doubled with all else held constant, does the reaction rate double? In other words, the reaction rate normalized to the number of surface sites (TOF) or catalyst loading (norm. rate or STY) is expected to be constant for a reaction free of transport artifacts.[83] We routinely observe a constant TOF (rate/$[*]_o$) within experimental error for reaction rates that exhibit first-order dependence on sites as surface metal oxide coverage is increased from say 1 V/nm^2 to a monolayer coverage of 8 V/nm^2, including reactions discussed in Figure 3a,b. The caveat being that data are collected at differential reaction conditions of low reactant conversion, low catalyst loadings, small particle diameters, etc. However, under the same differential reaction conditions aimed at minimizing transport artifacts using the same catalysts, reactions where the rate exhibits second-order dependence on $[*]_o$, shown in Figure 3c−e, do not evince constant TOF. In such cases, TOF increases linearly as the metal oxide coverage increases, unless the reaction rate is normalized by the square of sites (rate/$[*]_o^2$). Therefore, we believe that such nuances need to be kept in mind when applying the Madon-Boudart test to kinetic data collected via well-designed experiments under the differential reaction regime to prevent misattribution of underlying chemistry and mechanistic information to transport artifacts.

Other groups have also reported examples of heterogeneously catalyzed reactions exhibiting $r \propto [*]_o^2$. For example, the steady state rate of this reaction over Cu-SSZ-13 catalysts was shown to exhibit second-order dependence on Cu sites.[84] Specifically, a pioneering report on the mechanism of the low-temperature SCR of NO with NH_3 over Cu-SSZ-13 catalysts elegantly demonstrated that, during the oxidation half cycle in these catalysts, if O_2 oxidant (necessitating a 4-electron exchange) was used, the reaction exhibited a second-order dependence on Cu site density.[85] On the other hand, if NO_2 (2-electron exchange) was used an oxidant instead of O_2 during the oxidation half cycle, the reaction exhibited first-order dependence on the number of Cu site density on the same catalysts, presumably due to the unimolecular nature of the rate-determining step when NO_2 is oxidizing the Cu^1 species. These findings are in line with the analysis shown in Figure 3, where 2 electron oxidation reactions typically exhibit a first-order dependence on the number of active sites, while oxidations involving ≥4 electrons tend to exhibit second-order dependence on the total number of active sites, owing to the higher demands of the >4 electron oxidations necessitating two sites and subsequent slow steps, or a single bimolecular rate-determining step.

Beyond the examples discussed in the preceding sections, we also note that compelling experimental evidence against the necessity of "pair sites" assumed in the earlier heterogeneous catalysis literature can be gleaned from other literature studies reporting specific mechanisms that enable nonadjacent sites to conduct bimolecular reactions.[86] For example, remote, isolated sites have been shown to interact and communicate with each other via long-range transfer of electrons[87,88] or tunneling of hydrogen species such as protons, neutral atoms, and hydride ions during acid−base reactions and proton-coupled electron transfer reactions on solid catalysts.[89−94] Other mechanisms known to operate in heterogeneous catalysis that enable a long-range interaction between remote catalytic sites, enabled by the interaction of reactants or products with the solid catalyst, include shuttling of protons and hydroxyl ions via surface PO_x sites in phosphate-containing materials[95−98] and shuttling of protons assisted by water adducts within zeolite pores.[99,100] Water-assisted proton shuttling has also been reported for nonzeolite materials, including supported Pd catalysts,[101] mesoporous silica,[102,103] etc., suggesting the widespread relevance of such long-distance interaction mechanisms in heterogeneous catalysis. In summary, the examples highlighted

https://doi.org/10.1021/acscatal.4c02813
ACS Catal. 2024, 14, 10260−10270

herein and the possible underlying catalytic mechanisms that enable nonadjacent sites to function provide strong motivation to be wary of idealized assumptions behind oft-invoked models when faced with contradictory experimental data.

4. OUTLOOK

It is almost trite to point out that global kinetic models like L-H/L-H-H-W do not provide much information regarding the underlying surface mechanisms of heterogeneous catalysts. In Boudart's own words:

> *"...kinetic data—necessary as they may be—will usually remain insufficient. They must be bolstered by spectroscopic data that define the composition and structure of the catalyst, and all intermediates involved in the elementary steps that constitute the catalytic reaction."*[4]

However, as most of us who have been involved in heterogeneous catalysis research will agree, over the years, countless reports have been published where researchers rely on fitting global kinetic models to experimental rate data with the objective of acquiring molecular insights into the surface mechanism. Not only that but also these studies do so without taking into account the nuances of those global kinetic models, the assumptions behind their derivation, the complexities of heterogeneous catalyst surfaces, the surface sites, surface reaction mechanisms, etc. Through this perspective, our objective is to highlight the unique advantages and complexities of supported metal oxide catalysts that consist of active two-dimensional surface metal oxides and allow for differentiating how idealized models like L-H/L-H-H-W should be applied to these catalysts in order to prevent confusion and controversy.

Herein, we revisit the oft-invoked L-H model for bimolecular surface reactions, which was derived for metal catalysts with the a priori assumption of immobile adsorbates reacting on neighboring pair sites, such that the rate varies linearly with the total number of active sites $\left(r \propto \frac{Z}{2}[*]_o^{\,1}\right)$. We first categorically show that, even in model single crystal metal catalysts, immobile adsorbates are not present on adjacently located pair sites due to facile surface diffusion, as elegantly shown by *in situ* STM of NO dissociation on the Ru(0001) surface by Ertl et al.[12] Moving to supported metal oxide catalysts, the assumption fails once again, as HAADF-TEM and MAS NMR of supported VO_x catalysts do not evince any regularly arranged pair sites, especially at low loadings in submonolayer coverages of the active supported metal oxide phase. Moreover, microscopic and spectroscopic characterization of supported metal oxide catalysts, including supported VO_x, demonstrate that, unlike metal catalysts, supported metal oxide catalysts allow systematic variation in the surface site density via metal oxide loading in the submonolayer surface coverage region. We then analyze a wide range of reactions catalyzed by supported VO_x catalysts in terms of the dependence of the reaction rate on the number of total surface VO_x sites. The rates of reaction for methanol oxidation, oxidative dehydrogenation of propane, oxidative dehydrogenation of ethane, SO_2 oxidation to SO_3, etc. were all found to exhibit a linear dependence on the total number of surface VO_x sites in submonolayer covered supported vanadium oxide catalysts because they all involve a unimolecular rate-determining step requiring only one catalytic active site. On the other hand, the rates of reaction for selective catalytic reduction of NO with NH_3, propylene oxidation to acrolein, *n*-butane oxidation to maleic anhydride, etc. were found to exhibit a quadratic dependence on the total number of VO_x surface sites for submonolayer supported vanadium oxide catalysts because these reactions involve a bimolecular rate-determining step requiring at least two catalytic active surface sites. Based on our analysis, we propose that a more appropriate treatment of the L-H model would be to not make any a priori assumptions about the nature of active sites (nuclearity, local arrangement, surface site density, etc.) or the nature of the adsorbates (mobile, immobile, molecularly adsorbed or dissociatively adsorbed, etc.) and allow carefully collected experimental data to elucidate kinetics as a function of number of active surface sites, adsorbate coverage, etc. Via this simple treatment of the L-H model, the rate is expected to vary with the surface site density, i.e., $r \propto [*]_o^{\,n}$, where $n = 1$ or 2 for rate-determining steps being unimolecular and bimolecular or two separate sites participating in slow steps, respectively. For bimolecular rate-determining steps, the probability of two mobile adsorbates or surface metal oxide sites combining/colliding to form the product scales nonlinearly with the total number of sites, irrespective of the surface site nuclearity, thereby, introducing the requirement for $n > 1$. Our analysis further implies that kinetic analysis, free of the assumption of pair sites arranged in a symmetric lattice, can allow one to differentiate between surface reaction mechanisms based on the surface site requirements. For example, the rate dependence on $[*]_o$ can be used to distinguish between bimolecular reactions occurring via an E-R mechanism involving reaction between a gas phase reactant and a surface adsorbate, where $r \propto [*]_o^{\,1}$ vs a L-H mechanism, where $r \propto [*]_o^{\,2}$ if the rate-determining step is a bimolecular surface reaction.

AUTHOR INFORMATION

Corresponding Authors

Daniyal Kiani − *Renewable Resources and Enabling Sciences Center, National Renewable Energy Laboratory, Golden, Colorado 80401, United States*; Email: daniyal.kiani@nrel.gov

Israel E. Wachs − *Operando Molecular Spectroscopy and Catalysis Laboratory, Department of Chemical and Biomolecular Engineering, Lehigh University, Bethlehem, Pennsylvania 18015, United States*; orcid.org/0000-0001-5282-128X; Email: iew0@lehigh.edu

Complete contact information is available at: https://pubs.acs.org/10.1021/acscatal.4c02813

Notes

The authors declare no competing financial interest.

ACKNOWLEDGMENTS

D.K.'s contribution was supported in part by the National Renewable Energy Laboratory (NREL), operated by Alliance for Sustainable Energy, LLC, for the U.S. Department of Energy (DOE) under Contract No. DE-AC36-08GO28308. This work was supported by the Director's Fellowship - Laboratory Directed Research and Development (LDRD) Program at NREL. The views expressed in the article do not necessarily represent the views of the DOE or the U.S. Government. The U.S. Government retains and the publisher, by accepting the article for publication, acknowledges that the U.S. Government retains a nonexclusive, paid-up, irrevocable, worldwide license to publish or reproduce the published form of this work, or allow others to do so, for U.S. Government purposes. I.E.W.'s contribution was supported by the U.S. National Science Foundation (NSF) under award # CBET-2221714.

https://doi.org/10.1021/acscatal.4c02813
ACS Catal. 2024, 14, 10260−10270

REFERENCES

(1) Hougen, O. A.; Watson, K. M. General Principles. *Industrial & Engineering Chemistry* **1943**, *35* (5), 529−541.
(2) Yang, K. H.; Hougen, O. A. Determination of mechanism of catalyzed gaseous reactions. *Chemical engineering progress* **1950**, *46* (3), 149−157.
(3) Boudart, M. Chapter 7 - Heterogeneous Catalysis. In *Reaction in Condensed Phases*; Eyring, H., Ed.; Academic Press, 1975; pp 349−411.
(4) Boudart, M.; Djéga-Mariadassou, G. *Kinetics of Heterogeneous Catalytic Reactions*; Princeton University Press, 1984.
(5) Boudart, M. Four Decades of Active Centers. *American Scientist* **1969**, *57* (1), 97−111.
(6) Hougen, O. A.; Watson, K. M. *Chemical process principles*; John Wiley & Sons, Inc., 1943.
(7) Wachs, I. E. Progress in catalysis by mixed oxides: From confusion to catalysis science. *Catal. Today* **2023**, *423*, No. 113883.
(8) Thomas, J. M.; Thomas, W. J. *Introduction to the principles of heterogeneous catalysis*; Academic Press, 1967.
(9) Vannice, M. A. *Kinetics of Catalytic Reactions*; Springer, 2005.
(10) Davis, M. E.; Davis, R. J. *Fundamentals of chemical reaction engineering*; McGraw-Hill Higher Education, 2003.
(11) Chorkendorff, I.; Niemantsverdriet, J. W. *Concepts of modern catalysis and kinetics*; John Wiley & Sons, 2017.
(12) Zambelli, T.; Wintterlin, J.; Trost, J.; Ertl, G. Identification of the "Active Sites" of a Surface-Catalyzed Reaction. *Science* **1996**, *273* (5282), 1688−1690.
(13) Zhou, W.; Ross-Medgaarden, E. I.; Knowles, W. V.; Wong, M. S.; Wachs, I. E.; Kiely, C. J. Identification of active Zr−WOx clusters on a ZrO2 support for solid acid catalysts. *Nat. Chem.* **2009**, *1* (9), 722−728.
(14) Wachs, I. E. Catalysis science of supported vanadium oxide catalysts. *Dalton Transactions* **2013**, *42* (33), 11762−11769.
(15) Kiani, D.; Sourav, S.; Baltrusaitis, J.; Wachs, I. E. Elucidating the Effects of Mn Promotion on SiO2-Supported Na-Promoted Tungsten Oxide Catalysts for Oxidative Coupling of Methane (OCM). *ACS Catal.* **2021**, *11* (16), 10131−10137.
(16) Kiani, D.; Sourav, S.; Wachs, I. E.; Baltrusaitis, J. Synthesis and molecular structure of model silica-supported tungsten oxide catalysts for oxidative coupling of methane (OCM). *Catalysis Science & Technology* **2020**, *10* (10), 3334−3345.
(17) Zhou, W.; Wachs, I. E.; Kiely, C. J. Nanostructural and chemical characterization of supported metal oxide catalysts by aberration corrected analytical electron microscopy. *Curr. Opin. Solid State Mater. Sci.* **2012**, *16* (1), 10−22.
(18) Jaegers, N. R.; Lai, J.-K.; He, Y.; Walter, E.; Dixon, D. A.; Vasiliu, M.; Chen, Y.; Wang, C.; Hu, M. Y.; Mueller, K. T.; et al. Mechanism by which Tungsten Oxide Promotes the Activity of Supported V2O5/TiO2 Catalysts for NOX Abatement: Structural Effects Revealed by 51V MAS NMR Spectroscopy. *Angew. Chem., Int. Ed.* **2019**, *58* (36), 12609−12616.
(19) Ruckenstein, E.; Lee, S. H. Effect of the strong metal-support interactions on the behavior of model nickel/titania catalysts. In *Wetting Experiments*; CRC Press, 2018; pp 292−311.
(20) Debecker, D. P.; Stoyanova, M.; Rodemerck, U.; Eloy, P.; Léonard, A.; Su, B.-L.; Gaigneaux, E. M. Thermal Spreading As an Alternative for the Wet Impregnation Method: Advantages and Downsides in the Preparation of MoO3/SiO2−Al2O3Metathesis Catalysts. *J. Phys. Chem. C* **2010**, *114* (43), 18664−18673.
(21) Jentoft, F. C.; Schmelz, H.; Knözinger, H. Preparation of selective catalytic reduction catalysts via milling and thermal spreading. *Appl. Catal. A: General* **1997**, *161* (1), 167−182.
(22) He, Y.; Zhang, J.; Polo-Garzon, F.; Wu, Z. Adsorbate-Induced Strong Metal−Support Interactions: Implications for Catalyst Design. *J. Phys. Chem. Lett.* **2023**, *14* (2), 524−534.
(23) Wang, C.-B.; Cai, Y.; Wachs, I. E. Reaction-Induced Spreading of Metal Oxides onto Surfaces of Oxide Supports during Alcohol Oxidation: Phenomenon, Nature, and Mechanisms. *Langmuir* **1999**, *15* (4), 1223−1235.
(24) Xiong, H.; Kunwar, D.; Jiang, D.; García-Vargas, C. E.; Li, H.; Du, C.; Canning, G.; Pereira-Hernandez, X. I.; Wan, Q.; Lin, S.; et al. Engineering catalyst supports to stabilize PdOx two-dimensional rafts for water-tolerant methane oxidation. *Nature Catalysis* **2021**, *4* (10), 830−839.
(25) Wegener, S. L.; Marks, T. J.; Stair, P. C. Design Strategies for the Molecular Level Synthesis of Supported Catalysts. *Acc. Chem. Res.* **2012**, *45* (2), 206−214.
(26) Gasior, M.; Haber, J.; Machej, T. Evolution of V2O5-TiO2 catalysts in the course of the catalytic reaction. *Appl. Catal.* **1987**, *33* (1), 1−14.
(27) Haber, J. *role of surfaces in the reactivity of solids* **1984**, *56* (12), 1663−1676.
(28) Spivey, J. J.; Agarwal, S. K.; Knözinger, H.; Taglauer, E. Toward supported oxide catalysts via solid-solid wetting. In *Catalysis*, Spivey, J. J., Agarwal, S. K., Eds.; Vol. *10*; The Royal Society of Chemistry, 1993.
(29) Wang, Y.; Rosowski, F.; Schlögl, R.; Trunschke, A. Oxygen Exchange on Vanadium Pentoxide. *J. Phys. Chem. C* **2022**, *126* (7), 3443−3456.
(30) Liu, Z.; Ji, W.; Dong, L.; Chen, Y. The incorporated dispersion of vanadium oxide and its influence on the textural properties of tetragonal ZrO2. *Mater. Chem. Phys.* **1998**, *56* (2), 134−139.
(31) Wachs, I. E. The generality of surface vanadium oxide phases in mixed oxide catalysts. *Appl. Catal. A: General* **2011**, *391* (1), 36−42.
(32) Ek, M.; Ramasse, Q. M.; Arnarson, L.; Georg Moses, P.; Helveg, S. Visualizing atomic-scale redox dynamics in vanadium oxide-based catalysts. *Nat. Commun.* **2017**, *8* (1), 305.
(33) Huang, Z.; Ma, S.; Qu, B.; Li, D.; Zhou, R. Migration and oxidation of vanadium atom and dimer supported on anatase TiO2(1 0 1) surface. *Appl. Surf. Sci.* **2021**, *565*, No. 150517.
(34) Carrero, C. A.; Schloegl, R.; Wachs, I. E.; Schomaecker, R. Critical Literature Review of the Kinetics for the Oxidative Dehydrogenation of Propane over Well-Defined Supported Vanadium Oxide Catalysts. *ACS Catal.* **2014**, *4* (10), 3357−3380.
(35) Zhu, M.; Lai, J.-K.; Tumuluri, U.; Ford, M. E.; Wu, Z.; Wachs, I. E. Reaction Pathways and Kinetics for Selective Catalytic Reduction (SCR) of Acidic NOx Emissions from Power Plants with NH3. *ACS Catal.* **2017**, *7* (12), 8358−8361.
(36) Burcham, L. J.; Wachs, I. E. The origin of the support effect in supported metal oxide catalysts: in situ infrared and kinetic studies during methanol oxidation. *Catal. Today* **1999**, *49* (4), 467−484.
(37) Owens, L.; Kung, H. H. The Effect of Loading of Vanadia on Silica in the Oxidation of Butane. *J. Catal.* **1993**, *144* (1), 202−213.
(38) Zhao, C.; Wachs, I. E. An Operando Raman, IR, and TPSR Spectroscopic Investigation of the Selective Oxidation of Propylene to Acrolein over a Model Supported Vanadium Oxide Monolayer Catalyst. *J. Phys. Chem. C* **2008**, *112* (30), 11363−11372.
(39) Nakasaka, Y.; Kanda, T.; Shimizu, K.-i.; Kon, K.; Shibata, G.; Masuda, T. Micropore diffusivities of NO and NH3 in Cu-ZSM-5 and their effect on NH3-SCR. *Catal. Today* **2019**, *332*, 64−68.
(40) Rozanska, X.; Fortrie, R.; Sauer, J. Oxidative Dehydrogenation of Propane by Monomeric Vanadium Oxide Sites on Silica Support. *J. Phys. Chem. C* **2007**, *111* (16), 6041−6050.
(41) Gruber, M.; Hermann, K. Elementary steps of the catalytic NOx reduction with NH3: Cluster studies on adsorbate diffusion and dehydrogenation at vanadium oxide substrate. *J. Chem. Phys.* **2013**, *138* (19), 194701.
(42) Lwin, S.; Wachs, I. E. Catalyst Activation and Kinetics for Propylene Metathesis by Supported WOx/SiO2 Catalysts. *ACS Catal.* **2017**, *7* (1), 573−580.
(43) Lwin, S.; Keturakis, C.; Handzlik, J.; Sautet, P.; Li, Y.; Frenkel, A. I.; Wachs, I. E. Surface ReOx Sites on Al2O3 and Their Molecular Structure−Reactivity Relationships for Olefin Metathesis. *ACS Catal.* **2015**, *5* (3), 1432−1444.
(44) Kondratenko, E. V.; Cherian, M.; Baerns, M.; Su, D.; Schlögl, R.; Wang, X.; Wachs, I. E. Oxidative dehydrogenation of propane over V/MCM-41 catalysts: comparison of O2 and N2O as oxidants. *J. Catal.* **2005**, *234* (1), 131−142.
(45) Sourav, S.; Wang, Y.; Kiani, D.; Baltrusaitis, J.; Fushimi, R. R.; Wachs, I. E. New Mechanistic and Reaction Pathway Insights for

https://doi.org/10.1021/acscatal.4c02813
ACS Catal. 2024, 14, 10260−10270

Oxidative Coupling of Methane (OCM) over Supported Na2WO4/SiO2 Catalysts. *Angew. Chem., Int. Ed.* **2021**, *60* (39), 21502−21511.
(46) Wachs, I. E.; Jehng, J.-M.; Deo, G.; Weckhuysen, B. M.; Guliants, V. V.; Benziger, J. B.; Sundaresan, S. Fundamental Studies of Butane Oxidation over Model-Supported Vanadium Oxide Catalysts: Molecular Structure-Reactivity Relationships. *J. Catal.* **1997**, *170* (1), 75−88.
(47) Grant, J. T.; Carrero, C. A.; Love, A. M.; Verel, R.; Hermans, I. Enhanced Two-Dimensional Dispersion of Group V Metal Oxides on Silica. *ACS Catal.* **2015**, *5* (10), 5787−5793.
(48) Peck, T. C.; Reddy, G. K.; Roberts, C. A. Monolayer supported CuOx/Co3O4 as an active and selective low temperature NOx decomposition catalyst. *Catalysis Science & Technology* **2019**, *9* (5), 1132−1140.
(49) Peck, T. C.; Reddy, G. K.; Jones, M.; Roberts, C. A. Monolayer Detection of Supported Fe and Co Oxides on Ceria To Establish Structure−Activity Relationships for Reduction of NO by CO. *J. Phys. Chem. C* **2017**, *121* (15), 8435−8443.
(50) Rodriguez, J. A.; Liu, P.; Graciani, J.; Senanayake, S. D.; Grinter, D. C.; Stacchiola, D.; Hrbek, J.; Fernández-Sanz, J. Inverse Oxide/Metal Catalysts in Fundamental Studies and Practical Applications: A Perspective of Recent Developments. *J. Phys. Chem. Lett.* **2016**, *7* (13), 2627−2639.
(51) Hamilton, N.; Wolfram, T.; Tzolova Müller, G.; Hävecker, M.; Kröhnert, J.; Carrero, C.; Schomäcker, R.; Trunschke, A.; Schlögl, R. Topology of silica supported vanadium−titanium oxide catalysts for oxidative dehydrogenation of propane. *Catalysis Science & Technology* **2012**, *2* (7), 1346−1359.
(52) Routray, K.; Zhou, W.; Kiely, C. J.; Wachs, I. E. Catalysis Science of Methanol Oxidation over Iron Vanadate Catalysts: Nature of the Catalytic Active Sites. *ACS Catal.* **2011**, *1* (1), 54−66.
(53) Kim, T.; Wachs, I. E. CH3OH oxidation over well-defined supported V2O5/Al2O3 catalysts: Influence of vanadium oxide loading and surface vanadium−oxygen functionalities. *J. Catal.* **2008**, *255* (2), 197−205.
(54) Rozanska, X.; Fortrie, R.; Sauer, J. Size-Dependent Catalytic Activity of Supported Vanadium Oxide Species: Oxidative Dehydrogenation of Propane. *J. Am. Chem. Soc.* **2014**, *136* (21), 7751−7761.
(55) Kube, P.; Frank, B.; Schlögl, R.; Trunschke, A. Isotope Studies in Oxidation of Propane over Vanadium Oxide. *ChemCatChem.* **2017**, *9* (18), 3446−3455.
(56) Chen, K.; Iglesia, E.; Bell, A. T. Kinetic Isotopic Effects in Oxidative Dehydrogenation of Propane on Vanadium Oxide Catalysts. *J. Catal.* **2000**, *192* (1), 197−203.
(57) Frank, B.; Dinse, A.; Ovsitser, O.; Kondratenko, E. V.; Schomäcker, R. Mass and heat transfer effects on the oxidative dehydrogenation of propane (ODP) over a low loaded VOx/Al2O3 catalyst. *Appl. Catal. A: General* **2007**, *323*, 66−76.
(58) Chen, K.; Khodakov, A.; Yang, J.; Bell, A. T.; Iglesia, E. Isotopic Tracer and Kinetic Studies of Oxidative Dehydrogenation Pathways on Vanadium Oxide Catalysts. *J. Catal.* **1999**, *186* (2), 325−333.
(59) Khaliullin, R. Z.; Bell, A. T. A Density Functional Theory Study of the Oxidation of Methanol to Formaldehyde over Vanadia Supported on Silica, Titania, and Zirconia. *J. Phys. Chem. B* **2002**, *106* (32), 7832−7838.
(60) Pieck, C. L.; Bañares, M. A.; Fierro, J. L. G. Propane oxidative dehydrogenation on VOx/ZrO2 catalysts. *J. Catal.* **2004**, *224* (1), 1−7.
(61) Chen, K.; Bell, A. T.; Iglesia, E. The Relationship between the Electronic and Redox Properties of Dispersed Metal Oxides and Their Turnover Rates in Oxidative Dehydrogenation Reactions. *J. Catal.* **2002**, *209* (1), 35−42.
(62) Shee, D.; Rao, T. V. M.; Deo, G. Kinetic parameter estimation for supported vanadium oxide catalysts for propane ODH reaction: Effect of loading and support. *Catal. Today* **2006**, *118* (3), 288−297.
(63) Viparelli, P.; Ciambelli, P.; Lisi, L.; Ruoppolo, G.; Russo, G.; Volta, J. C. Oxidative dehydrogenation of propane over vanadium and niobium oxides supported catalysts. *Appl. Catal. A: General* **1999**, *184* (2), 291−301.
(64) Al-Ghamdi, S. A.; de Lasa, H. I. Propylene production via propane oxidative dehydrogenation over VOx/γ-Al2O3 catalyst. *Fuel* **2014**, *128*, 120−140.
(65) Dunn, J. P.; Stenger, H. G.; Wachs, I. E. Oxidation of sulfur dioxide over supported vanadia catalysts: molecular structure − reactivity relationships and reaction kinetics. *Catal. Today* **1999**, *51* (2), 301−318.
(66) Gao, X.; Bañares, M. A.; Wachs, I. E. Ethane and n-Butane Oxidation over Supported Vanadium Oxide Catalysts: An in Situ UV−Visible Diffuse Reflectance Spectroscopic Investigation. *J. Catal.* **1999**, *188* (2), 325−331.
(67) Zabilska, A.; Clark, A. H.; Moskowitz, B. M.; Wachs, I. E.; Kakiuchi, Y.; Copéret, C.; Nachtegaal, M.; Kröcher, O.; Safonova, O. V. Redox Dynamics of Active VOx Sites Promoted by TiOx during Oxidative Dehydrogenation of Ethanol Detected by Operando Quick XAS. *JACS Au* **2022**, *2* (3), 762−776.
(68) Willi, R.; Roduit, B.; Koeppel, R. A.; Wokaun, A.; Baiker, A. Selective reduction of NO by NH3 over vanadia-based commercial catalyst: Parametric sensitivity and kinetic modelling. *Chem. Eng. Sci.* **1996**, *51* (11), 2897−2902.
(69) Skotte, J.; Rasmussen, S. B.; Mikolajska, E.; Bañares, M. A.; Ávila, P.; Fehrmann, R. Redox behaviour of vanadium during hydrogen−oxygen exposure of the V2O5-WO3/TiO2 SCR catalyst at 250°C. *Appl. Catal. B: Environmental* **2011**, *107* (3), 340−346.
(70) Hashim, B.; Khan, W. U.; Hantoko, D.; Nasser, G. A.; Sanhoob, M. A.; Bakare, A. I.; Govender, N. S.; Ali, S. A.; Hossain, M. M. n-Butane Oxidation to Maleic Anhydride: Reaction Mechanism and Kinetics Over VPO Catalyst. *Ind. Eng. Chem. Res.* **2024**, *63* (14), 5987−6002.
(71) Morselli, L.; Trifirò, F.; Urban, L. Study of the interaction of 1-butene with V2O5 and mixed vanadium and phosphorus oxides by means of temperature-programmed desorption. *J. Catal.* **1982**, *75* (1), 112−121.
(72) Zhao, C.; Wachs, I. E. Selective oxidation of propylene to acrolein over supported V2O5/Nb2O5 catalysts: An in situ Raman, IR, TPSR and kinetic study. *Catal. Today* **2006**, *118* (3), 332−343.
(73) Redlingshöfer, H.; Fischer, A.; Weckbecker, C.; Huthmacher, K.; Emig, G. Kinetic Modeling of the Heterogeneously Catalyzed Oxidation of Propene to Acrolein in a Catalytic Wall Reactor. *Ind. Eng. Chem. Res.* **2003**, *42* (22), 5482−5488.
(74) Lai, J.-K.; Wachs, I. E. A Perspective on the Selective Catalytic Reduction (SCR) of NO with NH3 by Supported V2O5−WO3/TiO2 Catalysts. *ACS Catal.* **2018**, *8* (7), 6537−6551.
(75) Stegmann, N.; Ochoa-Hernández, C.; Truong, K.-N.; Petersen, H.; Weidenthaler, C.; Schmidt, W. The Mechanism and Pathway of Selective Partial Oxidation of n-Butane to Maleic Anhydride Studied on Titanium Phosphate Catalysts. *ACS Catal.* **2023**, *13* (24), 15833−15840.
(76) Centi, G.; Trifiro, F.; Ebner, J. R.; Franchetti, V. M. Mechanistic aspects of maleic anhydride synthesis from C4 hydrocarbons over phosphorus vanadium oxide. *Chem. Rev.* **1988**, *88* (1), 55−80.
(77) Busca, G.; Centi, G.; Trifiro, F. n-Butane selective oxidation on vanadium-based oxides: Dependence on catalyst microstructure. *Appl. Catal.* **1986**, *25* (1−2), 265−272.
(78) Coulston, G. W.; Bare, S. R.; Kung, H.; Birkeland, K.; Bethke, G. K.; Harlow, R.; Herron, N.; Lee, P. L. The Kinetic Significance of V5+ in n-Butane Oxidation Catalyzed by Vanadium Phosphates. *Science* **1997**, *275* (5297), 191−193.
(79) Zhai, Z.; Getsoian, A. B.; Bell, A. T. The kinetics of selective oxidation of propene on bismuth vanadium molybdenum oxide catalysts. *J. Catal.* **2013**, *308*, 25−36.
(80) Deo, G.; Wachs, I. E. Reactivity of Supported Vanadium Oxide Catalysts: The Partial Oxidation of Methanol. *J. Catal.* **1994**, *146* (2), 323−334.
(81) Tian, H.; Ross, E. I.; Wachs, I. E. Quantitative Determination of the Speciation of Surface Vanadium Oxides and Their Catalytic Activity. *J. Phys. Chem. B* **2006**, *110* (19), 9593−9600.
(82) Zhao, Z.; Gao, X.; Wachs, I. E. Comparative Study of Bulk and Supported V−Mo−Te−Nb−O Mixed Metal Oxide Catalysts for

https://doi.org/10.1021/acscatal.4c02813
ACS Catal. 2024, 14, 10260−10270

Oxidative Dehydrogenation of Propane to Propylene. *J. Phys. Chem. B* **2003**, *107* (26), 6333−6342.
(83) Madon, R. J.; Boudart, M. Experimental criterion for the absence of artifacts in the measurement of rates of heterogeneous catalytic reactions. *Industrial & Engineering Chemistry Fundamentals* **1982**, *21* (4), 438−447.
(84) Gao, F.; Mei, D.; Wang, Y.; Szanyi, J.; Peden, C. H. F. Selective Catalytic Reduction over Cu/SSZ-13: Linking Homo- and Heterogeneous Catalysis. *J. Am. Chem. Soc.* **2017**, *139* (13), 4935−4942.
(85) Paolucci, C.; Khurana, I.; Parekh, A. A.; Li, S.; Shih, A. J.; Li, H.; Di Iorio, J. R.; Albarracin-Caballero, J. D.; Yezerets, A.; Miller, J. T.; et al. Dynamic multinuclear sites formed by mobilized copper ions in NOx selective catalytic reduction. *Science* **2017**, *357* (6354), 898−903.
(86) Kiani, D.; Baltrusaitis, J. A Spectroscopic Study of Supported-Phosphate-Catalysts (SPCs): Evidence of Surface-mediated Hydrogen-Transfer. *ChemCatChem.* **2021**, *13* (8), 2064−2073.
(87) Huang, Z.; Liang, J.-X.; Tang, D.; Chen, Y.; Qu, W.; Hu, X.; Chen, J.; Dong, Y.; Xu, D.; Golberg, D.; et al. Interplay between remote single-atom active sites triggers speedy catalytic oxidation. *Chem.* **2022**, *8* (11), 3008−3017.
(88) Shan, J.; Zheng, Y.; Qiao, S.-Z. Communication between active sites regulates heterogeneous catalysis. *Chem.* **2022**, *8* (11), 2897−2899.
(89) Matxain, J. M.; Huertos, M. A. Hydrogen Tunneling in Stoichiometric and Catalytic Reactions involving Transition Metals. *ChemCatChem.* **2023**, *15* (24), No. e202300962.
(90) Pan, Z.; Horner, J. H.; Newcomb, M. Tunneling in C−H Oxidation Reactions by an Oxoiron(IV) Porphyrin Radical Cation: Direct Measurements of Very Large H/D Kinetic Isotope Effects. *J. Am. Chem. Soc.* **2008**, *130* (25), 7776−7777.
(91) Lauderdale, J. G.; Truhlar, D. G. Large tunneling effects in the migration of chemisorbed hydrogen on a metal. *J. Am. Chem. Soc.* **1985**, *107* (15), 4590−4591.
(92) German, E. D.; Abir, H.; Sheintuch, M. A Tunnel Model for Activated Hydrogen Dissociation on Metal Surfaces. *J. Phys. Chem. C* **2013**, *117* (15), 7475−7486.
(93) Hakanoglu, C.; Hawkins, J. M.; Asthagiri, A.; Weaver, J. F. Strong Kinetic Isotope Effect in the Dissociative Chemisorption of H2 on a PdO(101) Thin Film. *J. Phys. Chem. C* **2010**, *114* (26), 11485−11497.
(94) Meisner, J.; Kästner, J. Atom Tunneling in Chemistry. *Angew. Chem., Int. Ed.* **2016**, *55* (18), 5400−5413.
(95) Kiani, D.; Baltrusaitis, J. Surface chemistry of hydroxyapatite for sustainable n-butanol production from bio-ethanol. *Chem. Catalysis* **2021**, *1* (4), 782−801.
(96) Yashima, M.; Kubo, N.; Omoto, K.; Fujimori, H.; Fujii, K.; Ohoyama, K. Diffusion Path and Conduction Mechanism of Protons in Hydroxyapatite. *J. Phys. Chem. C* **2014**, *118* (10), 5180−5187.
(97) Uskoković, V. The role of hydroxyl channel in defining selected physicochemical peculiarities exhibited by hydroxyapatite. *RSC Adv.* **2015**, *5* (46), 36614−36633.
(98) Wu, Z.; Wang, S.; Gao, D.; Hu, R.; Jiang, X.; Chen, G. Unveiling the origin of enhanced catalytic performance of CePO4/Pt for selective hydrogenation of nitroarenes. *J. Catal.* **2024**, *430*, No. 115313.
(99) Stanciakova, K.; Weckhuysen, B. M. Water−active site interactions in zeolites and their relevance in catalysis. *Trends in Chemistry* **2021**, *3* (6), 456−468.
(100) Liu, Q.; van Bokhoven, J. A. Water structures on acidic zeolites and their roles in catalysis. *Chem. Soc. Rev.* **2024**, *53* (6), 3065−3095.
(101) Huang, P.; Yan, Y.; Banerjee, A.; Lefferts, L.; Wang, B.; Faria Albanese, J. A. Proton shuttling flattens the energy landscape of nitrite catalytic reduction. *J. Catal.* **2022**, *413*, 252−263.
(102) Krishna, S. H.; Gounder, R. Molecular water provides a channel for communication between Brønsted acid sites in solid catalysts. *Chem. Catalysis* **2021**, *1* (5), 968−970.
(103) Li, G.; Wang, B.; Kobayashi, T.; Pruski, M.; Resasco, D. E. Optimizing the surface distribution of acid sites for cooperative catalysis in condensation reactions promoted by water. *Chem. Catalysis* **2021**, *1* (5), 1065−1087.

https://doi.org/10.1021/acscatal.4c02813
ACS Catal. 2024, 14, 10260−10270